

## Putative mechanisms of antitumor activity of cyano-substituted heteroaryles in HeLa cells

**Katja Ester**<sup>1\*</sup>, **Fran Supek**<sup>2</sup>, **Kristina Majsec**<sup>1</sup>, **Marko Marjanović**<sup>1</sup>, **David Lembo**<sup>3</sup>, **Manuela Donalisio**<sup>3</sup>, **Tomislav Šmuc**<sup>2</sup>, **Ivana Jarak**<sup>4</sup>, **Grace Kraminski-Zamola**<sup>4</sup> and **Marijeta Kralj**<sup>1</sup>

1 Division of Molecular Medicine, Ruđer Bošković Institute, Bijenička 54, HR-10000 Zagreb, Croatia

2 Division of Electronics, Ruđer Bošković Institute, Bijenička 54, HR-10000 Zagreb, Croatia

3 Department of Clinical and Biological Sciences, University of Turin, S. Luigi Gonzaga Medical School, 10043, Orbassano, Turin, Italy

4 Department of Organic Chemistry, Faculty of Chemical Engineering and Technology, University of Zagreb, Marulićev trg 18, HR-10000 Zagreb, Croatia

\* kester@irb.hr

Tel: +385 14571235

Fax: +385 14561010

### Keywords

Cyano-substituted heteroaryles, HeLa cells, Random Forest, Apoptosis, Cytoskeleton disruption, Antioxidants

### Abstract

Six recently synthesized cyano-substituted heteroaryles, which do not bind to DNA but are highly cytotoxic against the human tumor cell line HeLa, were analyzed for their antitumor mechanisms of action (MOA). They did not interfere with the expression of human papillomavirus oncogenes integrated in the HeLa cell genome, but they did induce strong G1 arrest and result in the activation of caspase-3 and apoptosis. A computational analysis was performed that compared the antiproliferative activities of our compounds in 13 different tumor cell lines with those of compounds listed in the National Cancer Institute database. The results indicate that interference with cytoskeletal function and inhibition of mitosis are the likely antitumor MOA. Furthermore, a second *in silico* investigation revealed that the tumor cells that are sensitive to the cyano-substituted compounds show differences in their expression of locomotion genes compared with that of insensitive cell lines, thus corroborating the involvement of the cytoskeleton. This MOA was also confirmed

experimentally: the cyano-substituted heteroaryles disrupted the actin and the tubulin networks in HeLa cells and inhibited cellular migration. However, further analysis indicated that multiple MOA may exist that depend on the position of the cyano-group; while cyano-substituted naphthiophene reduced the expression of cytoskeletal proteins, cyano-substituted thieno-thiophene-carboxanilide inhibited the formation of cellular reactive oxygen species.

## **Introduction**

The discovery of novel chemotherapeutics has become one of the most important goals of medicinal chemistry. Novel heterocyclic organic compounds have been widely studied as promising agents able to induce cancer cells to undergo one of several types of cell death, in particular, apoptosis [1,2]. Of their various cellular targets, these compounds interfere with cellular kinases as well as with the organization of the cytoskeleton, mainly via disruption of the tubulin network [3,4].

As part of our continuing search for potential anticancer agents derived from heterocyclic compounds, we previously synthesized novel heterocyclic quinolones with strong antitumor activities, including cyano- and N-isopropylamidino-substituted derivatives of benzo[*b*]thiophene-2-carboxanilides and benzo[*b*]thieno[2,3-*c*]quinolones [5], and cyano- and amidino-substituted derivatives of thieno[2,3-*b*]- and thieno[3,2-*b*]thiophene-2-carboxanilides and thieno[3',2':4,5]thieno- and thieno[2',3':4,5]thieno [2,3-*c*]quinolones [6]. In parallel, we also synthesized and characterized the antitumor activities of novel cyano- and amidino-substituted derivatives of naphtho-furans, naphtho-thiophenes, thieno-benzofurans, benzo-dithiophenes, and their acyclic precursors [7]. The prime objective of these studies was to create compounds with strong antiproliferative activity, primarily through the introduction of various cyano- and amidino- substituted derivatives that would increase the DNA-binding affinity of the lead compounds. However, one of the most striking, and unexpected, observations was the extreme selectivity of several cyano-substituted derivatives toward HeLa and HEp-2 cell lines, which were active within the submicromolar range. None of these cyano-derivatives bound to DNA. Although we obtained potent antiproliferative activity using various derivatives lacking a cyano-group [4-7], the observed perturbation of the cell cycle and cell death (apoptosis, necrosis, or mitotic catastrophe) was mainly attributed to DNA

intercalation and the DNA damage response; moreover, none of the compounds showed selective activity toward any of the other tumor cell lines screened.

Natural cyano-containing compounds, laetriles, have been used for decades as a form of alternative medicine to treat cancer patients. Their claimed anticancer effects are not supported by clinical data [8], although more descriptive *in vitro* studies are available that show their mechanisms of action to be cell cycle arrest and the induction of apoptosis [9-10]. On the other hand, detailed studies of cyano-substituted heterocycles indicate that the major antitumor mechanism of action occurs via the induction of apoptosis through the inhibition of tubulin polymerization, and SAR (structure-activity relationships) analysis confirms that the cyano group is essential for the induction of apoptosis and extreme cytotoxicity [11,12]. Similarly, various heteroarylacrylonitriles that disturb the cell cycle and induce apoptosis in tumor cells [13,14] were shown to be less effective when the cyano-group was removed [13].

Recently, Hranjec *et al* [15] reported high antitumor activity of 2-benzimidazolyl-3-N-methylpyrolyl-acrylonitrile in various tumor cell lines and a special selectivity of the compound toward HeLa cells. However, no evidence exists to date that could provide a possible explanation of the high sensitivity of HeLa cells to these compounds.

In the present study, we selected 6 cyano-substituted derivatives (Fig. 1) showing pronounced cytotoxicity and selectivity toward HeLa cells, and investigated their antitumor mechanisms of action in more detail. In order to confirm and substantiate our previous results, 13 tumor cell lines were screened using an MTT proliferation assay. The antiproliferative effects of two selected representative compounds, compounds **3** and **5** (Fig. 1), were further explored by determining whether cell cycle perturbations had occurred, assessed by flow cytometry. Strong G1 arrest was followed by massive cell death caused by the induction of apoptosis; this latter effect was thus further evaluated. The possibility that the selectivity of cyano-substituted heteroaryles for HeLa cells is based on their interference with HPV oncogenes (integrated into the HeLa cell genome) was also investigated.

The data obtained by MTT screening allowed us to compare the antiproliferative activities of the compounds tested on different cell lines with those listed in the National Cancer Institute's (NCI) database. Further insight into HeLa specificity was achieved by comparing the gene expression profiles of cyano-substituted heteroaryle-sensitive cell lines with those of the insensitive cell lines tested. Both studies helped to direct our investigation and to focus on the major possible targets of cyano-substituted heteroaryles, i.e. cytoskeletal proteins.

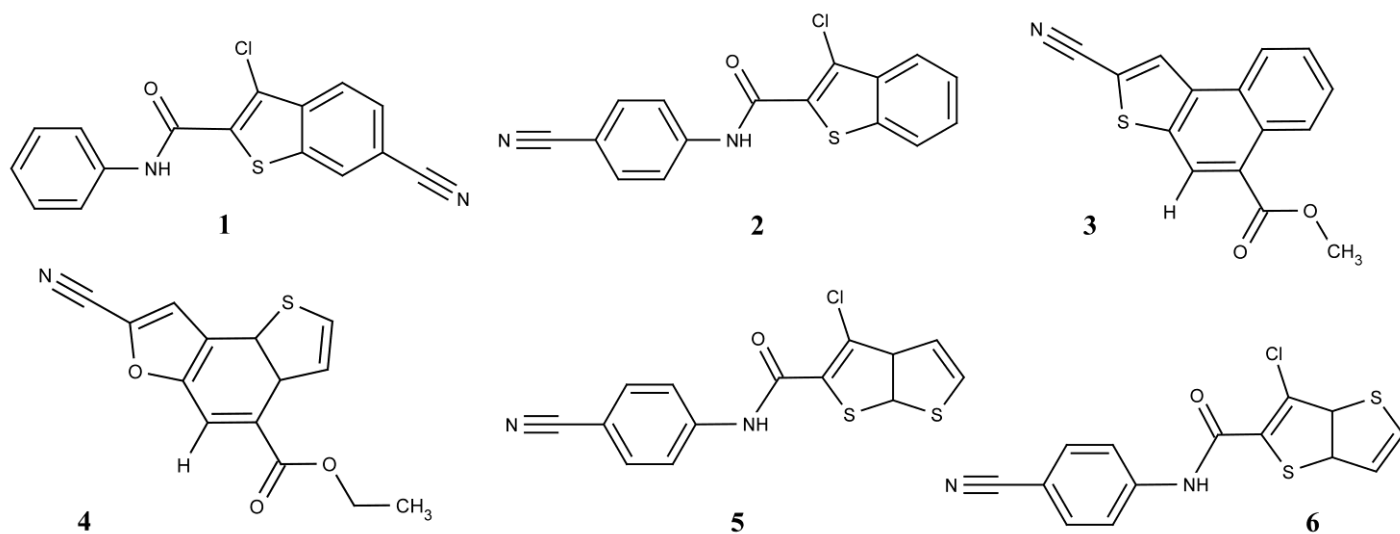


**Fig. 1** Structures of compounds under study.

## Material and methods

### Chemicals

The cyano-derivatives were synthesized as described earlier [5-7].

Fetal calf serum (FCS), Dulbecco's modified Eagle's medium (DMEM), penicillin–streptomycin (PS) and glutamine were purchased from GIBCO laboratories, Grand Island, NY. RPMI medium was purchased from Imunološki Zavod, Zagreb. Dimethyl sulfoxide (DMSO) and Formaldehyde were from Kemika, Zagreb. Antibodies against p27 (N-20), ERK 1 (K-23), p53 (DO-1), and PARP-1 (E-8) were purchased from Santa Cruz Biotechnology, Inc. Other antibodies used in this study were against: E- Cadherin, N-Cadherin and p-120 Catenin (all mice monoclonal, BD Transduction Laboratories, USA); p21 (mouse monoclonal, BD Pharmingen); Vimentin (mouse monoclonal, BioGenex, USA );  $\alpha$ -Tubulin (mouse monoclonal, Calbiochem). Secondary antibodies used were ECL Anti-mouse IgG/HRP (GE Healthcare Bio-Sciences Corp) and goat anti rabbit/HRP IgG (DakoCytomation, Denmark). Chemicals that were used for preparation of buffers and reagents, as well as control compounds used for various assays, were of the highest grade

commercially available and supplied by Sigma. Other chemicals used were specified elsewhere in the text.

#### Cell culture and antitumor activity assay

Antiproliferative activity was tested on the MiaPaCa-2 (pancreatic carcinoma), HEP-2 (laryngeal carcinoma), HeLa, SiHa, and Ca Ski (all cervical carcinoma), PC-3 (prostate carcinoma), HL-60 (acute promyelocytic leukemia), HT-29, HCT 116 and SW 620 (all colon carcinoma), H460 (lung carcinoma), MCF-7 (breast carcinoma), and MOLT-4 (acute lymphoblastic leukemia) tumor cell lines, obtained from American Type Culture Collection (ATCC, Rockville, MD, USA) All of the attached cells were cultured as monolayers and maintained in DMEM (an exception was PC-3 that was maintained in RPMI), while MOLT-4 and HL-60 cells were cultured in suspension in RPMI medium, all supplemented with 10% fetal calf serum (FCS), 2mM L-glutamine, 100 U/mL penicillin and 100 µg/mL streptomycin in a humidified atmosphere with 5% CO<sub>2</sub> at 37°C.

Growth inhibition activity was assessed as described previously, according to a slightly modified procedure of the National Cancer Institute, Developmental Therapeutics Program. The cells were inoculated onto standard 96-well microtiter plates on day 0 at  $3 \times 10^3$  to  $6 \times 10^3$  cells/well, depending on the doubling time of each cell line. Test agents were then added in five consecutive 10-fold dilutions ( $10^{-8}$ - $10^{-4}$  M) and incubated for further 72 h. Working dilutions were freshly prepared on the day of testing. The solvent (DMSO) was also tested for inhibitory activity by adjusting its concentration to the same as the working concentrations (maximal concentration of DMSO was 0.25%). Following 72 h of incubation, the cell growth rate was evaluated by performing the MTT assay, which detects dehydrogenase activity in viable cells. Absorbance (OD) was measured on a microplate reader at 570 nm. Each test point was performed in quadruplicate in three individual experiments. The results were expressed as GI<sub>50</sub>, which is the concentration necessary for 50% of inhibition. The GI<sub>50</sub> values for each compound were calculated from dose-response curves using linear regression analysis by fitting the test concentrations that gave PG values above and below the reference value (i.e. 50%). Each result was the mean value from three separate experiments.

### Flow cytometry for cell cycle Analysis

Tumor cells ( $2 \times 10^5$ ) were seeded per well into a 6-well plate. After 24 hours, compounds to be tested were added at  $1 \times 10^{-6}$  M concentrations. Following the desired length of time (24 h, 48 h and 72 h), attached cells were trypsinized, combined with floating cells, washed with phosphate buffer saline (PBS), and fixed with 70% ethanol and stored at  $-20^\circ\text{C}$ . Immediately before the analysis, the cells were washed with PBS and stained with  $50\mu\text{g/ml}$  of propidium iodide (PI) with the addition of  $0.2 \mu\text{g}/\mu\text{l}$  of RNase A. The stained cells were then analyzed with Becton Dickinson FACScalibur (Becton Dickinson) flow cytometer (20,000 counts were measured). The percentage of the cells in each cell cycle phase was determined using the ModFit LT™ software (Verity Software House) based on the DNA histograms. The tests were performed in duplicate and repeated at least twice.

### Flow cytometry for analysis of apoptosis

Detection and quantification of apoptotic cells at single cell level, was performed using Annexin V-Alexa 488 conjugate (Molecular Bioprobes, Invitrogen). The HeLa cells were seeded in 6-well plates ( $2 \times 10^5$  cells/well) and treated with compounds **3** and **5** at  $1 \times 10^{-6}$  M concentration. Following the desired length of time, both floating and attached cells were collected. The cells were then washed with PBS, pelleted and resuspended in the Annexin binding buffer (10 mM HEPES, 140 mM NaCl, 2,5 mM  $\text{CaCl}_2$ , pH 7,4) containing Annexin V-Alexa 488 conjugate, 7-actinomycin D (7-AAD, Molecular Bioprobes, Invitrogen). Camptothecin (10  $\mu\text{M}$ , Sigma) was used as the control apoptosis-inducing agent. The cells were then analyzed on Becton Dickinson FACScalibur flow cytometer (15,000 counts were measured). Fluorescence compensation and analysis were performed with FlowJo (TreeStar Inc.). Annexin V positive cells were determined to be early apoptotic and both Annexin V and 7-AAD positive cells were determined to be late apoptotic/necrotic cells.

### Caspase-3 colorimetric assay

Measurement of increased enzymatic activity of the caspase-3 class of proteases in apoptotic cells was performed using Caspase-3 Colorimetric Assay kit (R&D Systems, Inc.). The HeLa cells were seeded in 10 cm  $\varnothing$  Petri dishes ( $\sim 4$  dishes/ treatment,  $5 \times 10^5$  -  $1 \times 10^6$  cells/dish), to obtain  $\geq 2 \times 10^6$  cells/treated sample. After 24 h the compounds to be tested were added at

$1 \times 10^{-6}$  M concentration. Camptothecin (0.5  $\mu$ M, Sigma) was used as the control apoptosis-inducing agent. Following the desired length of time (as shown in the results section), attached cells were collected, pooled, washed with PBS, pelleted and lysed. The protein content of the cell lysate, which was about 4-10 mg/mL, was estimated using Lowry's method (Bio-Rad DCProtein Assay, Bio-Rad Laboratories) according to the manufacturer's recommendations. The enzymatic reaction for caspase activity was carried out for 2 h in a 96 well flat bottom microplate as recommended in the kit instructions, and OD was measured on a microplate reader at 405 nm. The reading value of each sample was normalized to the total protein content. Results are presented as histograms that represent mean values from the three separate experiments, where sample values were related to the control level, which was presented as 100%.

#### Inference of mechanistic class by comparison of cytostatic activity profiles across cell lines

These analyses were restricted to a subset of cell lines that also appear in the cell line screening database of the National Cancer Institute's Developmental Therapeutics Program (DTP-NCI): HT29, HCT-116, SW-620, MCF7, NCI-H460, PC-3, HL-60(TB) and MOLT-4. (The full DTP-NCI screening procedure consists of 60 cell lines). In order to integrate more accurately our in-house measurements with DTP-NCI data, we used a calibration procedure to eliminate systematic bias; this procedure has been previously described in detail [16]. Briefly, each of the eight cell lines listed above were treated with seven standard antitumor agents,  $GI_{50}$  values were calculated and linear regression used to relate the activities listed in the DTP-NCI database with our measurements, according to the function:  $GI_{50(DTP)} = a \cdot GI_{50(in-house)} + b$ , where constants  $a$  and  $b$  were determined for each cell line. In addition to the cell lines already calibrated [16], the same procedure was performed again using the HT29 cell line, giving  $GI_{50(HT29, DTP)} = 0.98 \cdot GI_{50(HT29, in-house)} + 0.53$  (correlation coefficient = 0.969;  $p=1.8 \cdot 10^{-4}$ ;  $p$ -value corrected for multiple tests using Holm's correction). A data set linking cytostatic compounds to a molecular mechanism of action (MOA) class was kindly provided by Dr. David Covell from DTP-NCI (personal communication) and then filtered as described in Supek et al [16]. The file containing  $GI_{50}$  measurements for DTP-NCI tested compounds was downloaded from [http://dtp.nci.nih.gov/docs/cancer/cancer\\_data.html](http://dtp.nci.nih.gov/docs/cancer/cancer_data.html) and processed as previously described [16]. Combining the two data sources resulted in a data set containing 514 compounds, each assigned to just one of the 12 possible MOA classes. The size of this set

of compounds (514) is slightly different to that previously reported (537) [16], as the panels of cell lines used differed slightly between the two analyses. In the current study, compounds were only included in the final dataset if they had  $\leq 2$  cell line measurements missing; for more details, see Supek et al [16]. Data were then standardized by subtracting the mean  $GI_{50}$  of a compound (calculated from tests on all cell lines) from each individual  $GI_{50}$  measurement and dividing by the standard deviation; in other words, the mean  $GI_{50}$  for each compound was adjusted to 0 and the standard deviation to 1. This MOA dataset is available on the authors' website at <http://anticancer.irb.hr/>. After extraction and preprocessing, the  $GI_{50}$  response data were analyzed by the Parallel Random Forest (PARF) software, an open-source implementation of the Random Forest (RF) algorithm. The RF classifier [17] is a data mining method based on an ensemble of decision tree models that map observations about an item ('attributes'; here  $GI_{50}$  values for cell lines) to conclusions about the item's target value ('class'; here the MOA) by recursively splitting the data into subsets based on an attribute value test; for more information, refer to the original RF paper [17]. PARF was run with the 'forest size' parameter set to a large value (10000 trees). The predictive performance of the RF classification model was estimated using the 'out-of-bag' cross-validation procedure [17] and is given in Table 4, along with the RF model's MOA predictions for the cyano-compounds tested.

In order to investigate which compounds from the dataset with known MOA compounds **3** and **5** are closest to (in terms of their cytostatic activity pattern across cell lines), we employed the principal components (PC) analysis technique, as implemented in the XLStat 2010 software (Addinsoft, Paris, France). In brief, it allows high-dimensional data (here: eight cell lines/dimensions) to be visualized on a two dimensional plot, while retaining as much information from the original measurements as possible. Consequently, the DTP-NCI compounds that are closest to compounds **3** and **5** in the PC plot also have the most similar cytotoxicity profiles for each of the eight cell lines. The PC plot was created from standardized  $\log GI_{50}$  values (see above) for the 19 compounds belonging to the 'mitotic agent' class, plus compounds **3** and **5**, using the XLStat 2010 software. In this case, the first two PCs together captured over half (51.4%) of the variance in the original data. PCs are dimensionless linear combinations of  $\log GI_{50}$  values of different cell lines and do not have a direct interpretation. Here, PC1 correlates well with the  $\log GI_{50}$  of NCI-H460 ( $r=0.90$ ), HCT-116 ( $r=0.62$ ) and HT29 ( $r=0.52$ ), while it anti-correlates with the  $\log GI_{50}$  of MOLT-4 ( $r=-0.74$ ), HL-60 ( $r=-0.63$ ) and SW-620 ( $r=-0.52$ ). PC2 correlates well with the  $\log GI_{50}$  of the PC-3 cell line ( $r=0.92$ ) and anti-correlates with the  $\log GI_{50}$  of MCF7 ( $r=-0.57$ ).

## Differentially expressed genes between sensitive and resistant cell lines

To complement the computational analysis of MOA class from cell line cytotoxicity profiles, we turned to an independent source of information that would provide insight into the mechanism behind the biological activity of the cyano-substituted heteroaryles. We downloaded a large dataset of human gene expression data (Affymetrix HG-U133A platform) that contained 1142 microarray measurements pertaining to human cell lines; the dataset is available from EBI ArrayExpress, accession number E-TABM-185. We selected 34 microarray measurements obtained from cell lines also used in our experiments and that were not exposed to any significant disruption of their optimal growth conditions; these mostly corresponded to the negative control conditions used in the various experiments composing the database. Of these, 12 samples belonged to the cell lines sensitive to the cyano-substituted compounds (8 samples for HeLa, and 4 samples for HEP-2), while the other 22 belonged to the insensitive cell lines (4 samples for MCF-7, 3 for SW-620, 8 for HT-29, 3 for PC-3, 4 for HL60, and 1 for MOLT4). Each sample contained readings from 22283 microarray probes; the task was to determine which of these probes (and their corresponding genes) carry information useful for discerning the sensitive from the resistant cell lines, i.e. which of the genes are differentially expressed between the two cell line categories. To this end, we used the Random Forest 'attribute importance' feature, as implemented in the PARF software. See Breiman L [17] for a description of the algorithm, Diaz-Uriarte and Alvarez de Andrés [18] for an application of RF for attribute selection on microarray data, and Strobl et al. [19] for recent refinements of this methodology. We set the PARF "forest size" (-n) parameter to 30000, and "the number of attributes to split on" (-m) parameter to 1000, and re-ran PARF five times with different random seeds to account for between-run variability in choosing the relevant probes; the most significant result (i.e. the lowest  $p$ -value) from the five runs was used to rank the probes. Six hundred and seventy-six probes had minimum values ( $p < 0.001$ ), equivalent to an RF attribute Z-score  $\geq 3.1$ , and thus could be considered to correlate with the sensitivity of the cell lines with compounds **3** and **5**. Taking into account (a) the noisiness of microarray data, and (b) the relatively low number of measurements compared to the number of probes, these estimates of sensitivity/expression correlation may not be reliable on a per-gene level. Therefore, we decided not to analyze the top 10, or any other list of differentially expressed genes, any further. Instead, to obtain a more robust result, we summarized the entire list of 676 differentially expressed probes by analyzing their cluster enrichment in (i)

Gene Ontology categories, (ii) 'cancer gene expression modules' [20], and (iii) sets of Reactome interactions, using the L2L Web server [21]. The full lists of differentially expressed probes and the Gene Ontology categories enriched with them are available on the authors' website <http://anticancer.irb.hr/>; the results with *p*-values <0.001 and enrichment > 2x are given in Table 5.

#### Quantification of HPV-18 E6 and E7 transcripts

Total RNA isolation was performed using a NucleoSpin II kit (Macherey-Nagel, Düren, Germany), and 2 µg of RNA were retrotranscribed with a RevertAid cDNA Synthesis Kit (Fermentas, Ontario, Canada). The resulting cDNAs were quantified by real-time PCR using the following primers: HPV-18 E6 forward primer 5'-TGGTGTATAGAGACAGTATACCCCA-3', HPV-18 E6 reverse primer 5'-GCCTCTATAGTGCCCAGCTATGT-3', HPV-18 E7 forward primer 5'-CCGAGCACGACAGGAACGACT-3', HPV-18 E7 reverse primer 5'-TCGTTTTCTTCTCTGAGTCGCTT-3', β-actin forward primer 5'-GTTGCTATCCAGGCTGTG-3', β-actin reverse primer 5'-TGTCCACGTCACACTTCA-3'. DNA amplifications were carried out using the Brilliant SYBR Green QPCR Master MIX (Stratagene) in a 96-well reaction plate format in a Mx3000P Real-Time Machine PCR System (Stratagene). The results were normalized to the β-actin levels, and compared with untreated controls which were set to 1.

#### Migration of cells

Cells were seeded at  $10^6$  per 10 cm ø Petri dish. After 24 h, compounds to be tested and the mitotic inhibitor Colchicine (Sigma) were added, as shown in the results section. Following 24 h of incubation, both floating and attached cells were collected, and washed in PBS. The percentage of viable cells was determined using Trypan blue (Sigma) staining. Transwell chambers for 24-well plates that contain membrane inserts with 8.0 µm pores (BD Biosciences) were inserted into each well. The cells resuspended in DMEM without FCS, but contained 0.1 % BSA (Sigma), were added onto membrane inserts, while DMEM with FCS was added into each well below the inserts. The cells were allowed to migrate to the undersides of the membranes for 18 h at 37°C in a CO<sub>2</sub> incubator. Membranes were washed with PBS, cells remaining on the upper sides of the membranes were removed using a cotton

swab, and then the migrated cells were fixed in 4 % formaldehyde for 15 min. The cells were stained with 0.5% Crystal violet and washed. The bottom of the chambers that contains cells attached to the membranes was excised and placed onto microscope glass slides, and cells were counted. The results from at least two separate experiments were used to determine percentage of migrating cells compared to untreated controls.

#### Western blot analysis

Cells were seeded at  $0.5 \times 10^6$  per 10 cm  $\varnothing$  Petri dish and treated after 24 h with 1  $\mu$ M concentration of compounds to be tested. After a desired length of time, cells were collected and lysed using lysis buffer (50 mM Tris pH 7,6, 150 mM NaCl, 2 mM EDTA, 1% Nonidet P40, 0,5% Triton X-100) with protease inhibitors (Roche) for 10 min on ice. Cell debris was pelleted by centrifugation at 13,200 rpm, 4 °C for 10 min. About 30  $\mu$ g of cytosolic proteins, as estimated by Lowry's method, were separated on 12% (or 8% where needed) sodium dodecyl sulfate polyacrylamide gel electrophoresis (SDS-PAGE) and transferred to a nitrocellulose membrane. For visualization of proteins and as an additional loading control, membranes were stained with Amido Black solution (Sigma) [22]. After destaining, membranes were blocked with 5% non-fat skimmed milk powder (Nestle) in Tris-buffered saline, and incubated with primary antibodies overnight at 4°C. The blots were washed with Tris-buffered saline Tween-20 (TBST) on a shaker and incubated for 90 min with secondary antibody tagged with horseradish peroxidase. After washing with TBST for 30 min, selected proteins were detected by SuperSignal West Pico Chemiluminescent substrate (Pierce Biotechnology, USA) or Western Lightning Chemiluminescent substrate (PerkinElmer LAS, Inc., USA).

#### Cellular tubulin staining

HeLa cells ( $0.5 \times 10^6$  /well) were grown overnight on 18 mm  $\times$  18 mm coverslips placed in each well of a six-well plate. Compounds to be tested, along with the tubulin inhibitors Paclitaxel (Sigma) and Colchicine (Sigma), were then added as described in the results section. After 24 h, the coverslips were washed with PBS and the cells fixed in 4% formaldehyde in PBS for 10 min, washed twice with PBS, and permeabilized with 0.1% Triton-X 100 in PBS for 10 min. The coverslips were than washed with PBS and blocked with 4% FCS in PBS for 30 min. After that, coverslips were incubated with anti- $\alpha$ -tubulin

antibody, washed in PBS, and incubated with FITC-goat antimouse IgG/IgM secondary antibody (BD Pharmingen) for 1 h. After being washed with PBS, each coverslip was washed with water and placed on a microscope slide in 1 drop of fluorescence mounting medium (DAKO). DAPI (Sigma)(4',6-diamidino-2-phenylindole), a fluorescent stain that binds to DNA, was added to the mounting medium in a final concentration of 100 ng/mL. Immunofluorescence was analyzed on an Olympus BX51 microscope with an Olympus DP51 camera.

### Cellular actin staining

HeLa cells ( $0.5 \times 10^6$  /well) were grown overnight on 18 mm  $\times$  18 mm coverslips placed in each well of a six-well plate. Compounds to be tested, along with the control actin inhibitors Cytochalasin B (Sigma) and Latrunculine B (Sigma), were then added as described in the results section. Following 24 h of incubation, the coverslips were washed and permeabilized as described for tubulin staining. The cells were incubated with Alexa fluor 594 phalloidin (Invitrogen) for 15 min in the dark. After washing with PBS, slides were prepared and analyzed as described for cellular tubulin staining.

### Measurement of cellular reactive oxygen species (ROS) production

Cellular ROS production was examined using 2',7'-dichlorofluorescein diacetate (DCFH-DA, Fluka), a nonfluorescent probe for intracellular ROS detection. The probe remains nonfluorescent inside a cell until its acetate groups have been removed by intracellular esterases and oxidized by intracellular ROS to the fluorescent compound 2',7'-dichlorofluorescein (DCF) [23]. HeLa cells ( $5 \times 10^3$ /well) were seeded into 96-well plates. Cells were washed with Hanks' Balanced Salt Solution (HBSS, GIBCO) and treated with 10  $\mu$ M DCFH-DA for 30 min at 37°C. The compounds tested were then added in four consecutive 10-fold dilutions ( $10^{-8}$ - $10^{-5}$ M) and the cells incubated for 2, 4, and 6 h. Fluorescence intensity was read with a Cary Eclipse Fluorescence Spectrophotometer (Varian) with an excitation wavelength of 500 nm and emission detection at 530 nm. The fluorescence intensities of the treated samples are presented as percentages of untreated control levels, set to 100%, and were obtained from at least three separate experiments performed in triplicate.

## Results

### Effect of cyano-compounds on the growth of various tumor cell lines

In order to confirm and substantiate our previous results [5-7], compounds **1-6** were screened on a panel of 13 tumor cell lines (Table 1). The antiproliferative activity of each compound in MiaPaCa-2, HEp-2, HeLa, SW620, and MCF-7 cell lines was reconfirmed, as was their selectivity toward HeLa and HEp-2 cells. Further cell lines, not included in the original screening (PC-3, HCT 116, H460, HT-29, MOLT-4, and HL-60), were introduced to allow comparison with the NCI screening platform. Two additional cervical carcinoma cell lines, SiHa and CaSki, were included to investigate the possibility that the high sensitivity of HeLa cells to these compounds might be related to oncogenic transformation by HPV E6 and E7 viral oncogenes. Interestingly, none of these newly introduced cell lines, including the cervical carcinomas, were as sensitive to the cyano-compounds as HeLa cells were; when tested in HeLa cells, the  $GI_{50}$  of most compounds was in the submicromolar range. The PC-3 and HCT 116 cell lines were, however, slightly more sensitive than the other lines (Table 1). Since the HEp-2 cell line has been shown to be contaminated with HeLa cells, the compounds tested were expected to produce a similar effect in these cells [24].

Table 1. In vitro inhibition of compounds **1-6** on the growth on tumor cells

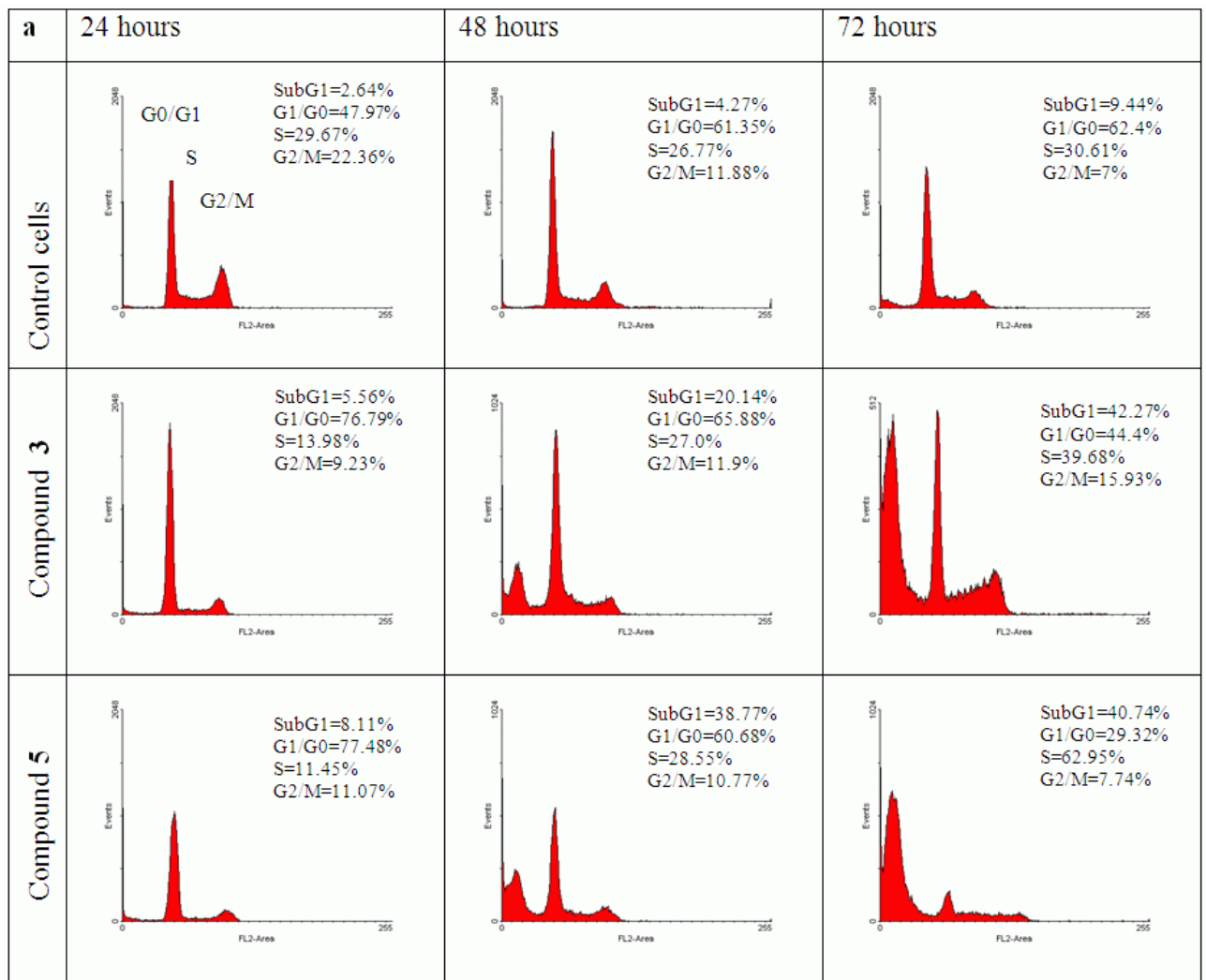
Compound <sup>b</sup>	GI <sub>50</sub> <sup>a</sup> (μM)												
	Cell lines												
	HEp-2	HeLa	MiaPaCa	CaSki	SiHa	MCF-7	SW620	HCT 116	H 460	PC3	HT 29	MOLT-4	HL-60
<b>1</b>	0.7±0.2	0.3±0.2	>100	>100	>100	>100	>100	33±45	>100	5±5	60±18	>100	>100
<b>2</b>	4±3.7	1.3±1	>100	>100	>100	>100	>100	>100	>100	2.5±0.3	>100	>100	>100
<b>3</b>	2±1	0.6±0.1	24±14	18±2	57±33	≥100	≥100	5±2	50±9	2.5±0.9	24±12	>100	>100
<b>4</b>	7±2	5.5±1.6	54±5	33±5	62±25	69±41	70±17	11±0.5	40±14	20±7	40±5	>100	32±6
<b>5</b>	0.6±0.2	0.3±0.2	>100	79±15	>100	>100	16±8	11±12	66±29	2±1	33±9	>100	>100
<b>6</b>	0.6±0.2	0.3±0.2	>100	≥100	≥100	≥100	≥100	>100	>100	4.0±1.0	>100	>100	>100

<sup>a</sup>GI<sub>50</sub>; the concentration that causes 50% growth inhibition

<sup>b</sup>See Fig. 1 for description of compounds

### Cell cycle perturbations by compounds **3** and **5**

Based on the strong antiproliferative activity of two structural representatives toward HeLa cells, compounds **3** and **5** were selected for further evaluation. Flow cytometric analysis showed that both compounds interfered with the cell cycle of HeLa cells, as shown in Fig. 2a. There were no differences between the compounds' effects following a 24 h exposure: cells were severely blocked in the G1 phase, while the numbers of cells in the S and G2/M phases were decreased. At this time point, cells showing reduced DNA content (subG1), indicative of apoptosis, were still absent, while at 48 h both compounds strongly elevated the subG1 fraction. As expected, a further increase in the percentage of the apoptotic cells was measured for both compounds following 72 h of treatment. Flow cytometric analysis of the cell cycle was also performed in MiaPaCa-2 cells (Fig. 2b). None of the tested compounds influenced the cell cycle at any of the 3 time points investigated.



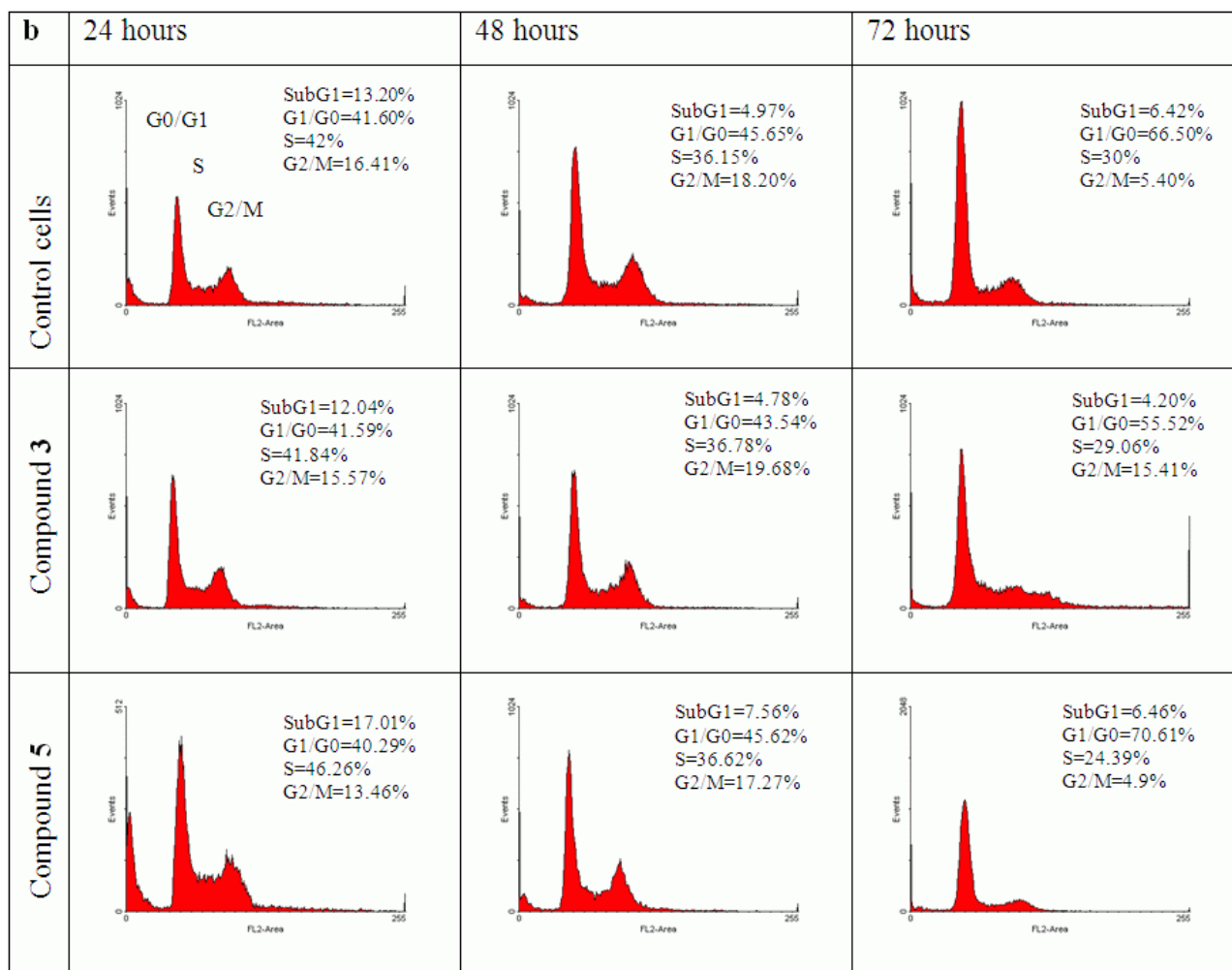


**Fig. 2** DNA histograms obtained by flow cytometry, and the percentages of cells (**a** HeLa and **b** MiaPaCa-2) in sub G1, G1, S and G2/M cell phase. Cells were treated with compounds **3** and **5** at  $10^{-6}$  M for 24h, 48 h and 72 h. Each presented histogram is a typical result, selected from at least two separate experiments performed in duplicates.

#### Changes in p21, p27, and p53 protein levels induced by compounds **3** and **5**

Since compounds **3** and **5** caused severe G1 arrest in HeLa cells (Fig. 2), protein levels of negative regulators of G1 progression, *i.e.* p21, p27, and, p53, were measured. Western blot analysis showed an increase in the p27 protein level following 24 h and 48 h of treatment with compound **3** (Fig. 3). Increased levels of p27 were only seen at the 48 h time point for compound **5**. An increased expression of p21 was obtained with compound **3** at 24 h, whereas reduced levels were observed with compound **5**. Neither of the compounds caused changes in the expression level of the p21 protein following 48 h of treatment. The protein levels of the tumor suppressor p53 were also investigated. Neither compound altered p53 expression, indicating that G1 arrest and apoptosis occur in a p53-independent manner (Fig. 3).

As the expression of tubulin is altered by treatment with compound **3** (discussed in more detail later on), total protein staining was performed using Amido Black, thus providing a more accurate loading control.

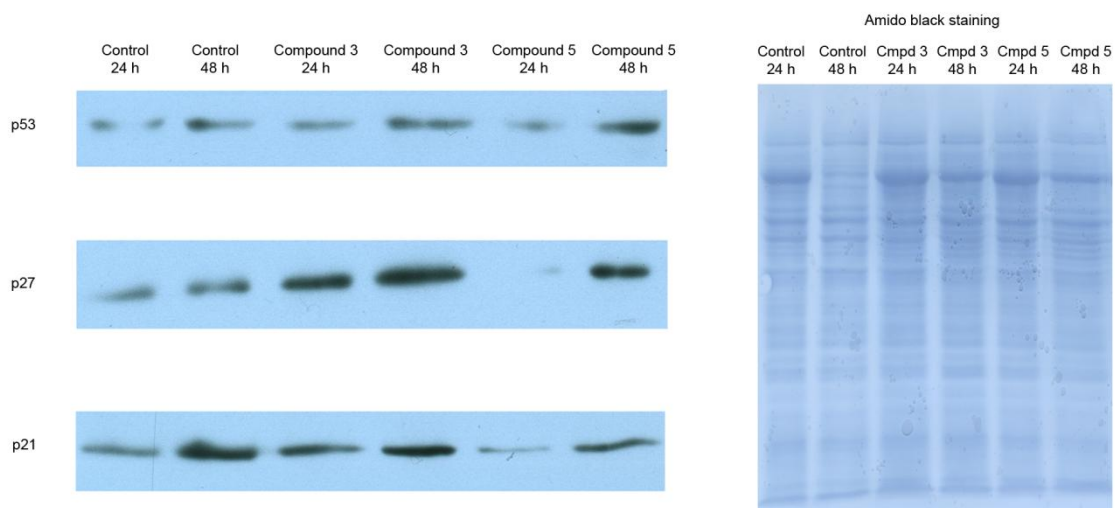


**Fig. 3** Western blot analysis of p21, p27 and p53 protein levels. HeLa cells were treated for 24h and 48 h with compounds **3** and **5** at 1 $\mu$ M. Cellular proteins (30  $\mu$ g) were separated on SDS gel electrophoresis and transferred onto a nitrocellulose membrane. Specific proteins were detected using antibodies for p21, p27 and p53, and total proteins were stained using Amido black. Blots are representatives from at least two separate experiments.

#### Effects of compounds **3** and **5** on induction of apoptosis

To further confirm and quantify the induction of apoptosis in HeLa cells by compounds **3** and **5**, an annexin-V assay was performed. Additional staining with 7-AAD, allowing the separation of the early from the late apoptotic/necrotic cells, confirmed a strong induction of apoptosis by both compounds (Table 2). A modest increase in the percentage of apoptotic cells following 24 h of treatment was followed by a severe induction following 48 h of treatment; compound **5** had a more pronounced effect at the 48 h time point than compound **3**. These results were also confirmed using an in-situ annexin-V assay (data not shown).

Table 2. Induction of apoptosis in HeLa cells by compounds **3** and **5** ( $10^{-6}$  M) measured by annexin-V assay

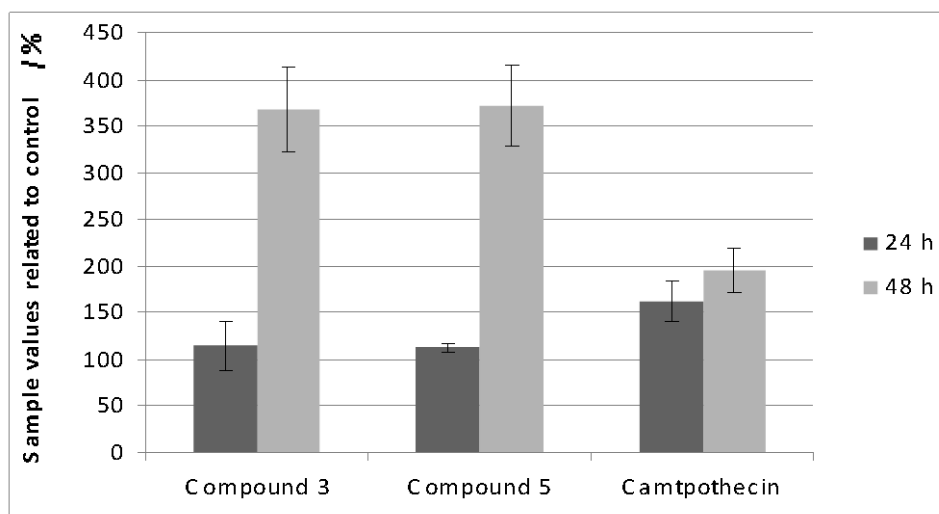
Treatment	Time (h)	Flow cytometry	
		Early apoptotic cells (%)	Late apoptotic/necrotic (%)
Control (DMEM)	24	4.1	2.3
	48	7.9	4.7
<b>3</b>	24	6.9	1.8
	48	16.1	12.8
<b>5</b>	24	6.8	2.2
	48	25.0	15.9

#### Involvement of caspase-3 and PARP-1 in apoptosis induced by compounds **3** and **5**

Caspase-3 activity. Given that a severe induction of apoptosis in HeLa cells was confirmed in the above experiments, the activity of caspase-3 was measured. Both compounds increased caspase-3 activity, but only following 48 h of treatment. Neither compound **3** nor compound **5** resulted in an increase in caspase-3 activity at the 24 h time point, while 0.5  $\mu$ M of Camptothecin, used as a positive control for apoptosis, did (Fig. 4a).

PARP-1 protein levels. Assessment of PARP-1 cleavage by a decrease in the level of uncleaved precursor was estimated by Western blot analysis (Fig. 4b). Compound **3** did not cause PARP-1 cleavage at any of the time points investigated, while the levels of PARP-1 uncleaved precursor were decreased following 48 h of treatment with compound **5**.

**a**



**b**

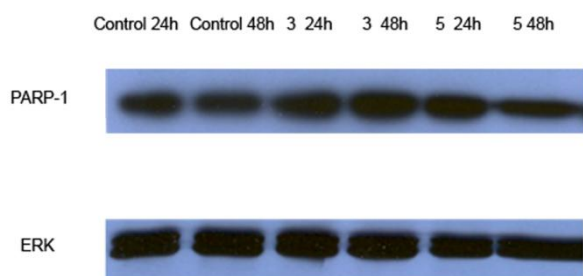


**Fig. 4** Role of caspase-3 and PARP-1 in apoptosis. HeLa cells were treated with compounds **3** and **5** ( $10^{-6}$  M) for 24 and 48 h, and then submitted to further analysis. **a** Histograms obtained by measurements of caspase-3 activity by Caspase-3 Colorimetric Assay. Each histogram represents mean values from the three separate experiments, where sample values were related to the control level, presented as 100%. **b** Western blot analysis of PARP-1 protein level. Cellular proteins (30  $\mu$ g) were separated on SDS gel electrophoresis and transferred onto a nitrocellulose membrane. The primary antibody used was specific for uncleaved precursor of PARP-1, and level of ERK 1 protein was used as the loading control. Blot is representative from at least two independent experiments.

## Interference with transcription of HPV-encoded oncogenes by selected cyano-substituted derivatives

To determine whether the selective antitumor actions of compounds **1**, **3**, and **5** correlate with the down-regulation of E6 and E7 mRNA levels, HeLa cells were treated with 1  $\mu$ M of each compound for 24 h and 48 h, and the E6 and E7 mRNA levels determined by real-time RT-PCR. The results, shown in Table 3, demonstrate that the compounds did not reduce the expression of E6 and E7 genes.

Table 3. Effect of cyano-substituted heteroaryles on the steady-state levels of HPV-18 E6 and E7 mRNAs in HeLa cells. HeLa cells were treated with 1  $\mu$ M of each compounds for 24 h and 48 h or left untreated. HeLa mRNA was retrotranscribed, and the levels of E6 and E7 transcripts were determined by real-time PCR. The results were normalized to the  $\beta$ -actin transcript levels. Results are shown as the mean  $\pm$  SD of three independent experiments.

<b>Compounds (1<math>\mu</math>M)</b>	<b>Relative E6 mRNA levels (mean values <math>\pm</math> SD)</b>	<b>Relative E7 mRNA levels (mean values <math>\pm</math> SD)</b>
<b>24 h</b>		
<b>Untreated</b>	1.00	1.00
<b>1</b>	1.18 $\pm$ 0.07	1.47 $\pm$ 0.18
<b>3</b>	1.35 $\pm$ 0.12	1.43 $\pm$ 0.24
<b>5</b>	0.98 $\pm$ 0.08	1.39 $\pm$ 0.15
<b>48 h</b>		
<b>Untreated</b>	1.00	1.00
<b>1</b>	1.29 $\pm$ 0.12	1.22 $\pm$ 0.14
<b>3</b>	1.22 $\pm$ 0.13	1.11 $\pm$ 0.09
<b>5</b>	1.06 $\pm$ 0.08	0.98 $\pm$ 0.07

## Computational investigation into the possible mechanisms of action

To investigate the putative mechanisms of action for cyano-substituted compounds, we drew upon two complementary sources of large-scale measurements of biological data: (i) the

database of cytostatic activity of various compounds at the DTP-NCI, and (ii) gene expression measurements by microarrays. Based on a classification of cell line activity profiles, the most likely mechanistic class for compounds **1**, **3**, **4**, and **5** was 'mitotic agents', i.e. drugs that interfere with mitosis by disrupting the cytoskeleton (Table 4). Compounds **3** and **5** presented similar activity profiles, and when compared with 19 previously described cytoskeleton-acting agents (Fig. 5), the activity profiles were most similar to some derivatives of colchicine (NSC33410, NSC335989) and some taxanes (NSC647752, Taxotere, NSC658831).

The study of microarray data revealed a number of genes that were differentially expressed in the cyano-substituted heteroaryle sensitive cell lines (HeLa, HEp-2) compared to the other insensitive cell lines investigated. The differentially expressed genes were found to be more frequent in particular gene groups, defined by: criteria of function, expression in cancer, or interaction partners (Table 5). The statistically highly significant results, which point to processes of cell motility and adhesion, and to localization in cell projections and the extracellular matrix, confirmed the hypothesis that compounds **3** and **5** act on the cytoskeleton or associated structures. On the other hand, we also noticed the appearance of genes related to – or interacting with – growth factors (insulin, IGF) and protein kinases (SRC). Interestingly, for cyano-substituted compounds **2** and **6**, the likely mechanistic class inferred from the cytostatic activity profiles was 'kinase agent' (Table 4), indicating the possibility that these two compounds might also interfere with cell signaling, although it is less likely than interference with the cytoskeleton.

Table 4. Performance estimates of a Random Forest (RF) classifier and its predictions for novel compounds. Average per-class precision and recall estimates of the RF model for determining MOA class were determined using out-of-bag crossvalidation. “Precision” is the proportion of drugs truly belonging to a class among all drugs predicted to have this class by the model. “Recall” is the proportion of all drugs of a certain class recognized as such by the model. Results for the cyano-substituted compounds (**1-6**) show the probability of belonging to each class; the highest probability is in bold.

Mechanistic class	Number of compounds	RF precision	RF recall	<b>1</b>	<b>2</b>	<b>3</b>	<b>4</b>	<b>5</b>	<b>6</b>
Alkylating agent	96	62.7%	77.1%	1.55%	6.38%	0.64%	0.74%	0.61%	8.34%
Antineoplastic antibiotic	40	53.1%	42.5%	1.41%	8.69%	2.75%	3.33%	2.07%	5.04%
Ion channel agent	19	76.5%	68.4%	5.85%	3.90%	7.85%	3.86%	3.53%	2.37%
DNA antimetabolite	34	71.0%	64.7%	11.39%	6.09%	13.30%	3.45%	11.23%	4.96%
Intercalating agent	87	57.5%	74.7%	7.48%	2.39%	2.98%	1.89%	23.66%	7.25%
Kinase agent	25	75.0%	60.0%	5.20%	<b>34.27%</b>	1.49%	0.92%	3.98%	<b>27.22%</b>
Membrane agent	44	63.6%	31.8%	10.62%	8.68%	4.19%	5.15%	7.56%	14.16%
Mitotic (cytoskeleton) agent	19	70.6%	63.2%	<b>47.59%</b>	9.47%	<b>43.18%</b>	<b>64.45%</b>	<b>36.30%</b>	17.31%
Nucleobase analog	44	71.1%	61.4%	6.86%	15.52%	22.37%	13.81%	5.07%	9.18%
Steroid	21	63.6%	66.7%	0.32%	0.33%	0.35%	1.01%	0.45%	0.21%
Topoisomerase I poison	41	60.4%	70.7%	0.07%	1.26%	0.11%	0.46%	0.19%	0.73%
Topoisomerase II poison	43	48.6%	39.5%	1.66%	3.02%	0.79%	0.93%	5.35%	3.23%

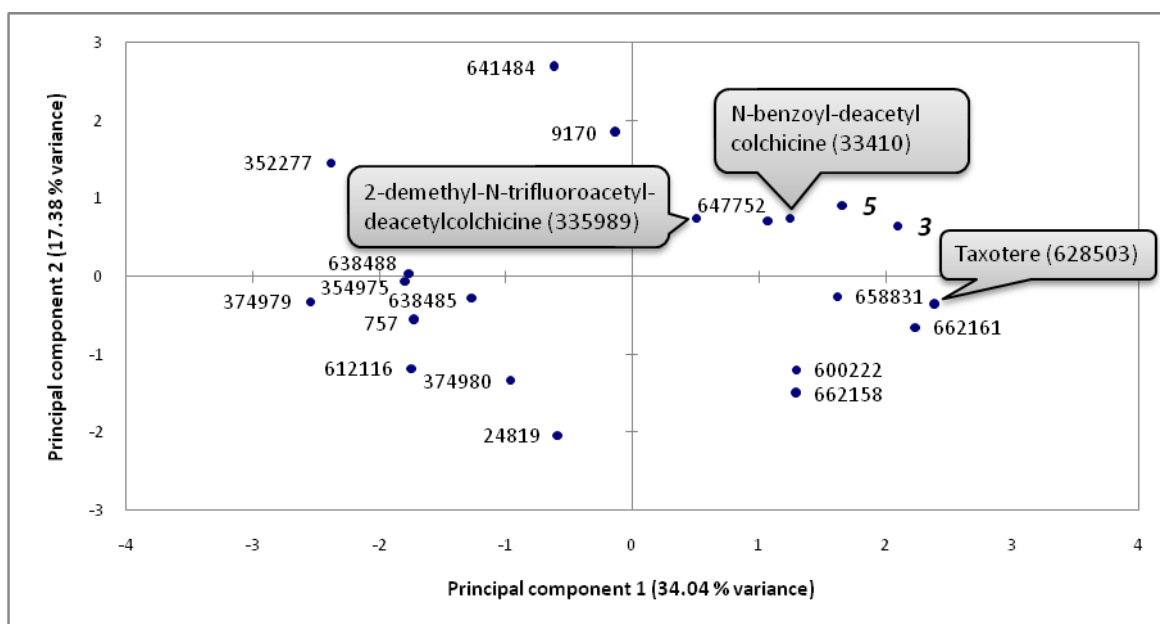


**Fig. 5** A principal component (PC) plot of 19 known antitumor agents in the 'mitotic agents' class, and the compounds **3** and **5**. The PCs were derived from standardized log GI<sub>50</sub> values (see Materials and Methods) for eight cell lines. PCs are dimensionless; See Material and Methods section for a possible interpretation of PC1 and PC2. Numbers adjacent to dots are the "NSC" identifier which can be used to find the compounds in the DTP-NCI databases, except for compounds **3** and **5**.

Table 5. Gene groups enriched with genes differentially expressed between cell lines sensitive (HeLa and HEP-2) and resistant (MCF-7, SW-620, HT-29, PC-3, HL60 and MOLT4) to compounds **3** and **5**.

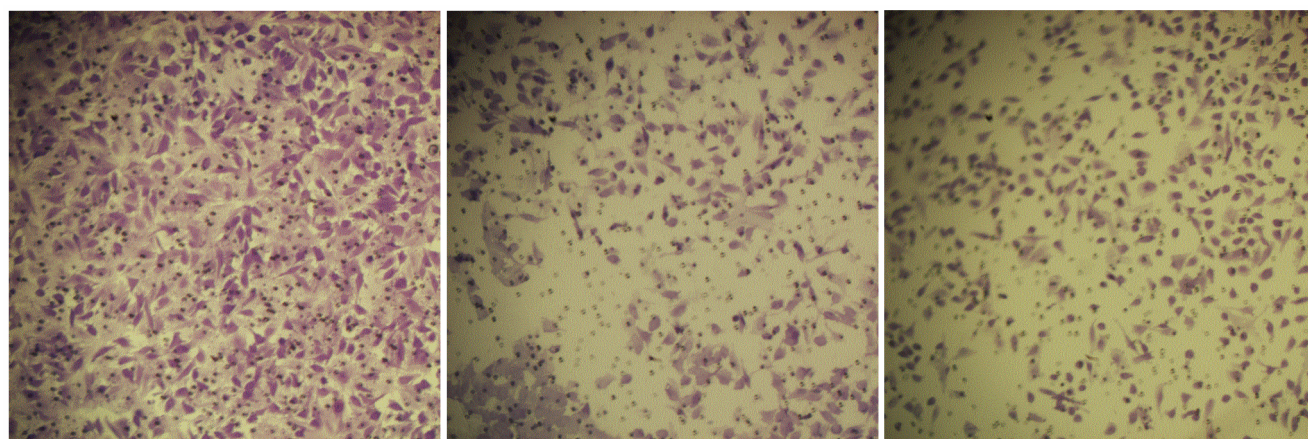
List Name	Description	Fold Enrichment	Binomial p-value
<b>Gene Ontology</b>			
positive regulation of cell motility	Any process that activates or increases the frequency, rate or extent of the movement of a cell.	6.79	1.89E-04
microvillus	Thin cylindrical membrane-covered projections on the surface of an animal cell containing a core bundle of actin filaments. Present in especially large numbers on the absorptive surface of intestinal cells.	7.4	1.12E-04
insulin-like growth factor binding	Interacting selectively with an insulin-like growth factor, any member of a group of polypeptides that are structurally homologous to insulin and share many of its biological activities, but are immunologically distinct from it.	7.98	2.67E-07
growth factor binding cyclin-dependent protein kinase inhibitor activity	Interacting selectively with any growth factor, proteins or polypeptides that stimulate a cell or organism to grow or proliferate. Stops, prevents or reduces the activity of a cyclin-dependent protein kinase.	3.39	6.81E-05
<b>Cancer Gene Expression Modules *</b>			
module_47	Module 47 (ECM and collagens)	3.01	6.02E-10
module_190	Module 190 (IGFBPs)	11.11	4.01E-08
module_474	Module 474 (untitled)	8.14	8.83E-07
module_551	Module 551 (untitled)	7.08	1.47E-04
module_384	Module 384 (adhesion molecules)	5.82	4.67E-04
module_515	Module 515 (untitled)	3.21	6.38E-04
<b>Reactome *</b>			
SRC	Reactome interactions for SRC	7.54	3.88E-04
INS	Reactome interactions for INS	7.14	5.11E-04
INSR	Reactome interactions for INSR	7.14	5.11E-04

\* Comprehensive information for specific Cancer Gene Expression modules [21] is available from <http://ai.stanford.edu/~erans/cancer/>

Effects of the compounds **3** and **5** on cell migration

The overall rate of HeLa cell migration following 24 h of treatment with compounds **3** and **5** was determined (Fig. 6); two different concentrations were investigated. Both compounds inhibited migration in a dose-dependent manner: neither of the compounds influenced migration at 0.5 $\mu$ M, while at 1 $\mu$ M the number of migrating cells was significantly reduced. To exclude an effect of cytotoxicity as the cause of reduced migration, cell viability was measured during each experiment; a survival rate of at least 80% confirmed that reduced migration was not attributable to cytotoxic effects of the compounds. As Colchicine has also been shown to inhibit the migration of fibroblasts [25], and Colchicine analogs have been shown to have similar activity profiles to compounds **3** and **5**, various concentrations of Colchicine were also evaluated in parallel for their effect upon HeLa cell migration. However, the concentrations of Colchicine that reduced the rate of cell migration were cytotoxic for HeLa cells (data not shown).

**a**



Control cells

Compound 3  
10<sup>-6</sup>M

Compound 5  
10<sup>-6</sup>M

**b**

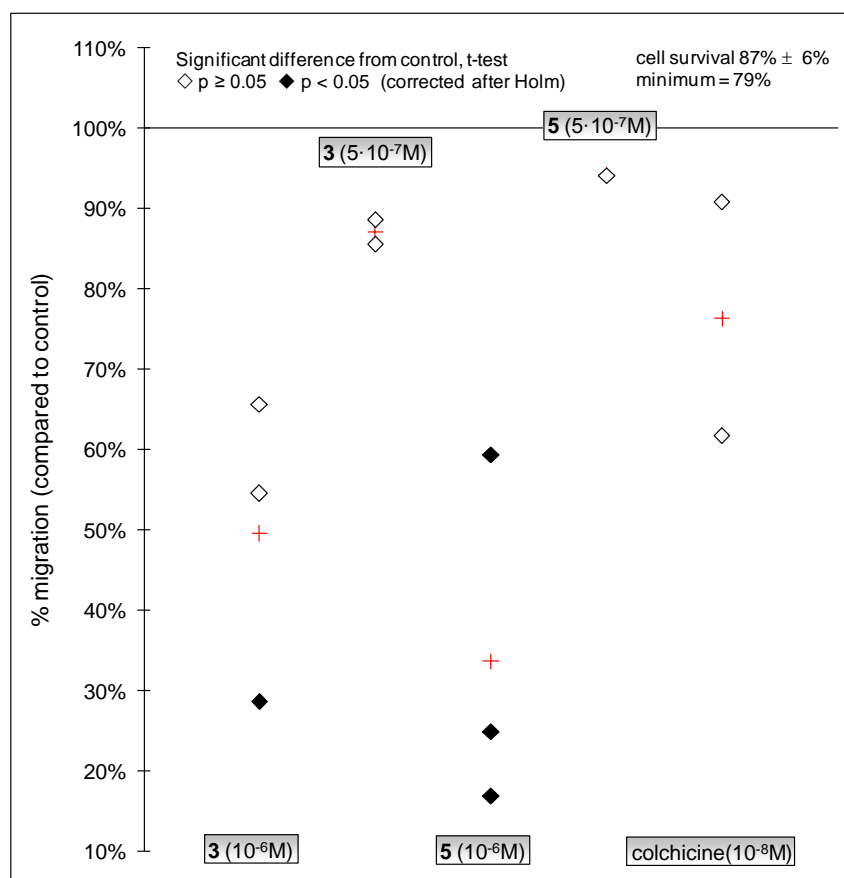
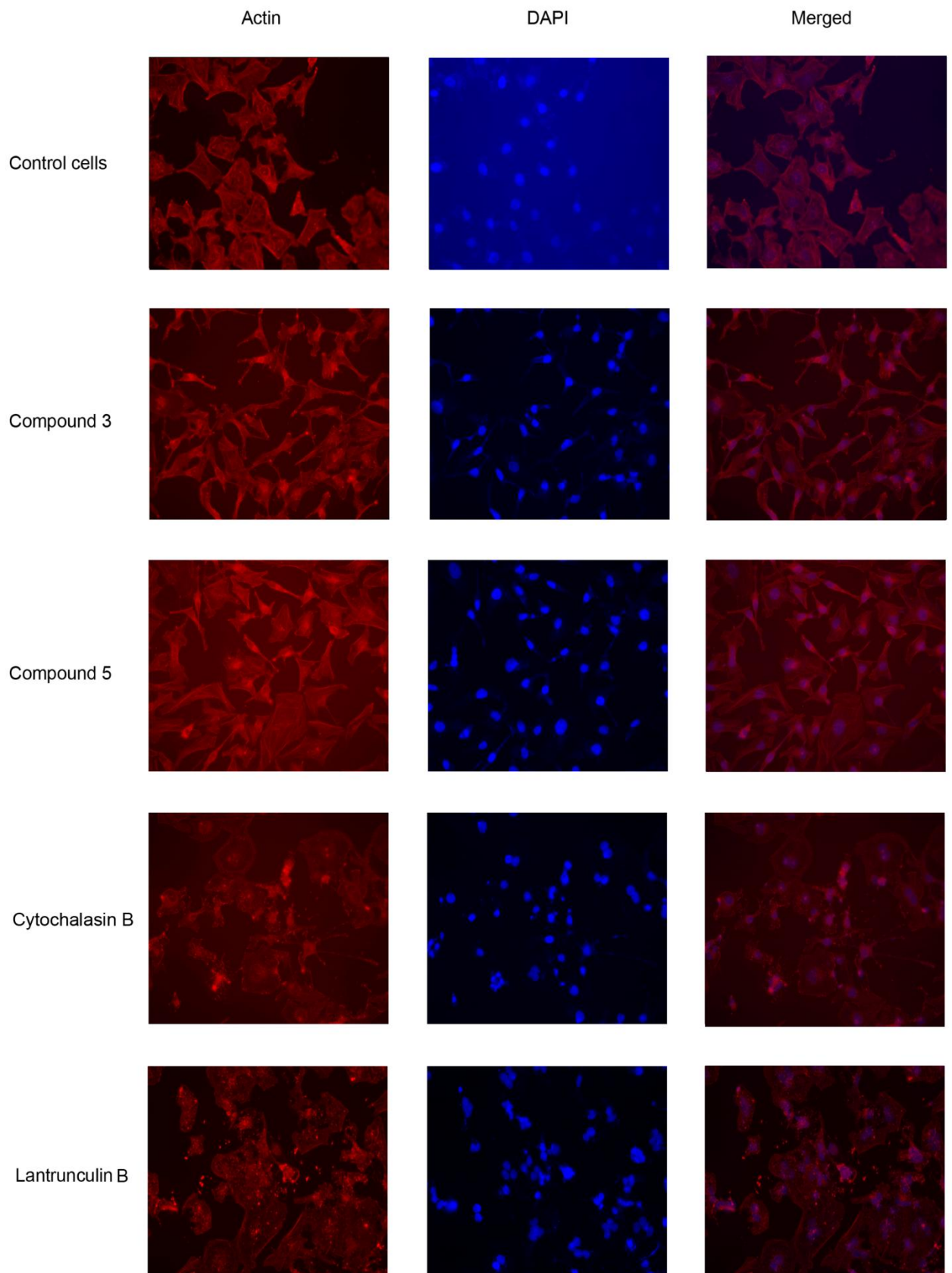


**Fig. 6** Migration of HeLa cells upon treatment with compounds **3** and **5**. Cells were exposed to compounds **3** and **5** at  $5 \times 10^{-7}$  M and  $1 \times 10^{-6}$  M for 24 h, and then allowed to migrate through a membrane inserts for 18 h. Migrated cells were stained, photographed (**a**) and counted. Number of migrated cells (**b**) was presented as a percentage of migrated cells compared to an untreated control.

#### Disruption of actin and tubulin networks by treatment with compounds **3** and **5**

To determine whether compounds **3** and **5** are able to disrupt the cellular cytoskeleton of HeLa cells composed of actin and tubulin filaments, cells were treated with compound **3** or **5** at 1  $\mu$ M concentration, stained and photographed. Although noticeable changes were not present following 24 h of treatment (data not shown), both compounds resulted in damage to the actin and tubulin networks 48 h post-treatment (Fig. 7). However, the observed changes did not resemble those visible after the exposure of cells to known inhibitors of actin (Cytochalasin B and Latrunculin B) or tubulin (Paclitaxel and Colchicine) (Fig. 7).

**a**



**b**

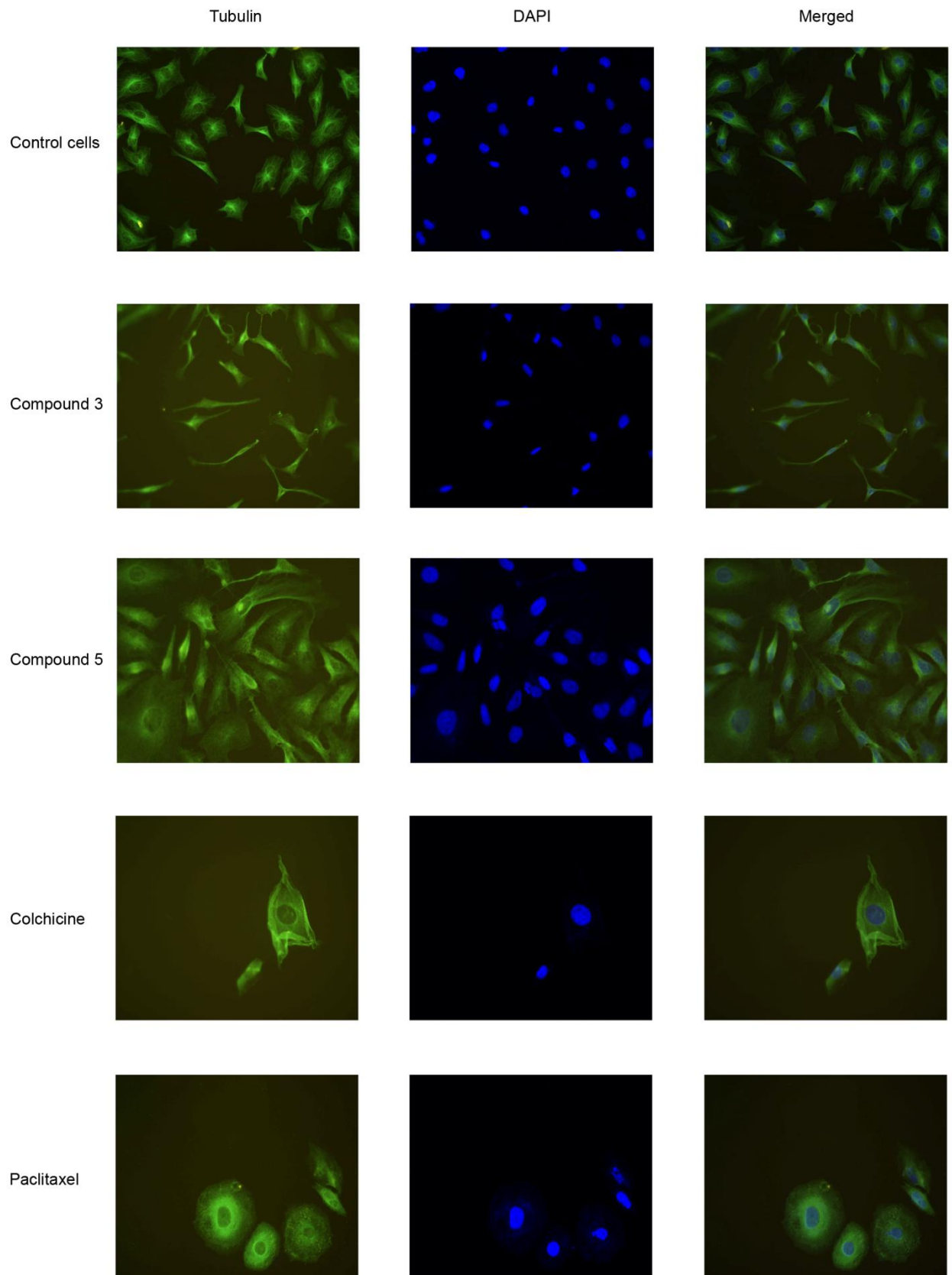


**Fig. 7** Cytoskeletal changes upon treatment of HeLa cells for 48 h with compounds **3** and **5** at 1  $\mu$ M. Cellular actin (**a**) was stained using phalloidin, and positive controls included Cytochalasin B and Latrunculine B at  $5 \times 10^{-6}$  M. Cellular tubulin (**b**) was stained using immunofluorescence and positive controls included Paclitaxel at  $10^{-8}$  M and Colchicine at  $10^{-7}$  M. DAPI was used to stain nuclei. Results are typical of three separate experiments.

Changes in the protein levels of E-cadherin, N-cadherin, p-120 catenin, vimentin, and  $\alpha$ -tubulin, induced by compounds **3** and **5**

To evaluate further the inhibition of cytoskeletal filaments by compounds **3** and **5**, changes in the protein levels of vimentin and  $\alpha$ -tubulin were determined following a 24 h exposure to the compounds. Differences in the expression of adhesion molecules, including various cadherins and p120-catenin, were also assessed. The results obtained by Western blot are presented in Fig. 8. Compound **3** reduced the expression of N-cadherin,  $\alpha$ -tubulin, and vimentin, while levels of p120-catenin and E-cadherin remained unchanged. Compound **5** did not change the expression level of any of the proteins investigated. The human keratinocyte cell line HaCaT (CLS, Germany) was included as a positive control for E-cadherin expression.

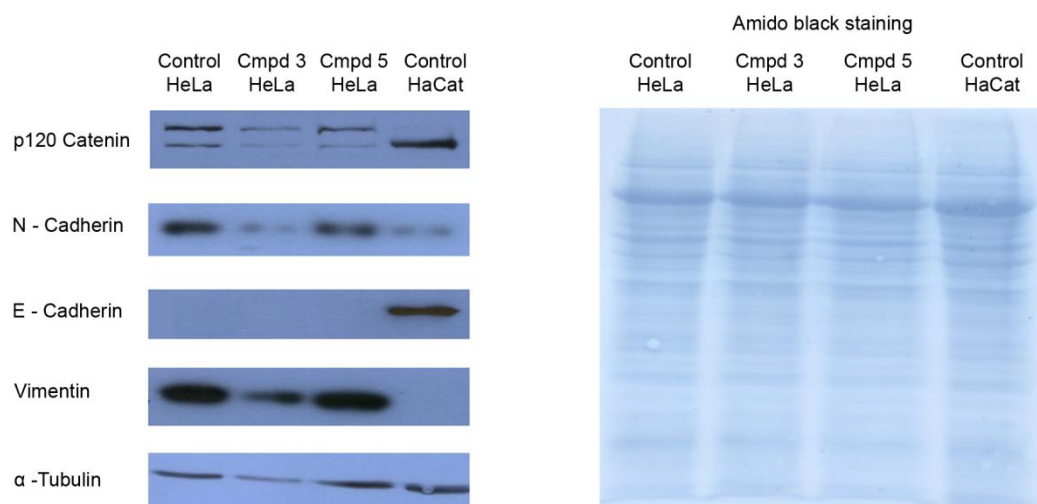


**Fig. 8** Effect of compounds **3** and **5** on the expression of E-cadherin, N-cadherin, p-120 catenin, vimentin and  $\alpha$ -tubulin. The cells were treated with 1  $\mu$ M concentration of each compound for 24 h. Cellular proteins (30  $\mu$ g) were separated on SDS gel electrophoresis and

transferred onto nitrocellulose membrane. Specific proteins were detected using monoclonal antibodies against E-cadherin, N-cadherin, p-120 catenin, vimentin and  $\alpha$ -tubulin, and total proteins were stained using Amido Black. Blots are representatives from at least two independent experiments.

#### Alteration in the formation of cellular ROS following treatment with compounds **3** and **5**

As shown in Fig. 9, both compounds decreased levels of cellular ROS in HeLa cells. This interesting effect began quickly and was already present at 2 h. However, due to the cytotoxic nature of compounds **3** and **5**, values of ROS at longer time points, i.e. 24 h and 48 h, could not be evaluated (data not shown). The data obtained using 1  $\mu$ M of compounds **3** and **5** are presented as it is the concentration closest to the compounds'  $GI_{50}$  values and used as the representative concentration across all experiments performed. As seen in Fig. 9, the antioxidant activity of compound **5** was stronger than that of compound **3**.

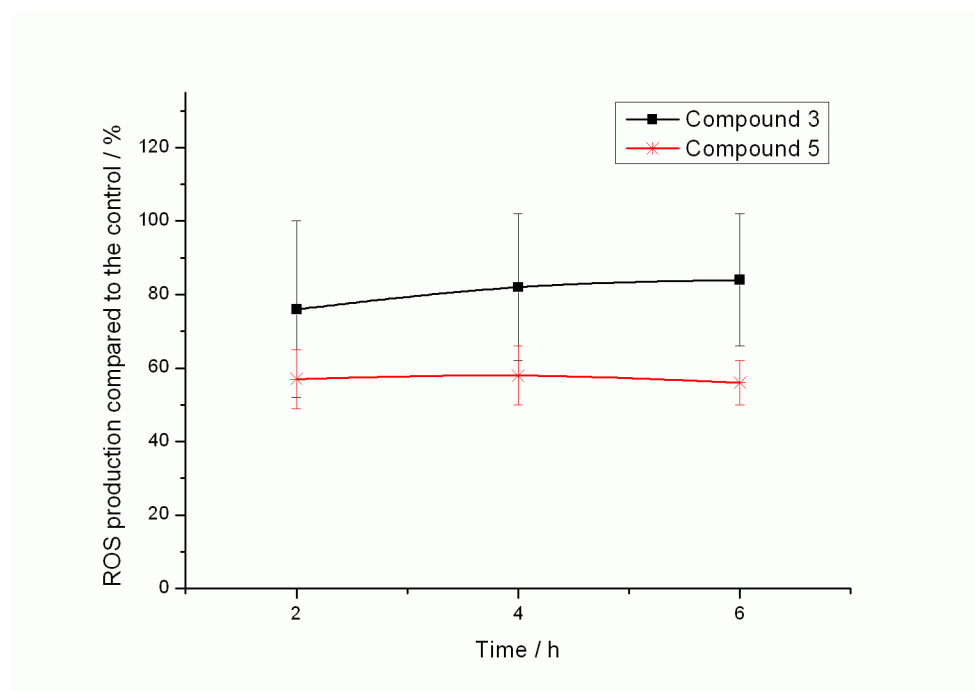


**Fig. 9** Time responsive ROS production by compounds **3** and **5**. Intracellular ROS production was measured in HeLa cells treated with 1  $\mu$ M of compounds **3** and **5** by using a nonfluorescent probe 2',7'-dichlorofluorescein diacetate. The data is presented as mean  $\pm$  SD of three independent experiments

## Discussion

The purpose of this study was to elucidate the antitumor mechanisms of action of recently synthesized cyano-substituted heteroaryles, primarily as an attempt to combine numerous interesting aspects of their effects.

Antiproliferative screening confirmed the selectivity of six compounds for the HeLa cell line. It was hypothesized that the particular sensitivity of HeLa cells toward these compounds was related to HPV oncogenic transformation. However, the antiproliferative activity of these compounds was only modest when tested in other HPV-transformed cells (CaSki and SiHa). Moreover, the treatment of HeLa cells with these compounds was not found to interfere with HPV-18 E6 and E7 oncogene transcription. One of the several mechanisms by which HPV transforms an infected cell [26] is via the inactivation of the p53 tumor suppressor by E6, which targets p53 for degradation. Possible restoration of p53 protein levels, anticipated in the case that the compounds interfere with viral oncogenes, was not found. The unchanged levels of p53 after treatment also suggest that all of the effects produced by the compounds, such as cell cycle disturbance and apoptosis, occurred in a p53-independent manner. In addition to the HeLa cell line, the PC-3 cell line was also affected by treatment with the cyano-substituted heteroaryles, although the  $GI_{50}$  was ten-fold higher for most compounds. Another cell line, HCT 116, also demonstrated a certain degree of sensitivity toward the compounds. Although both PC-3 and HeLa cells possess impairments in their p53 statuses, HCT 116 carries wild type p53, which suggests that sensitivity to the compounds investigated is not related to a cell's p53 status.

Cell cycle analysis revealed strong G1 arrest following a 24 h exposure of the cells to either compound **3** or **5** - the two representative compounds selected for further investigation in this study. In the case of compound **3**, the G1 arrest was accompanied by an increase in p21 and p27 protein expression, while a decrease in their levels accompanied treatment with compound **5**. This may suggest that compound **5** causes G1 arrest by affecting a distinct signaling pathway to compound **3**, which does not necessarily involve the inhibition of cyclin-dependent kinases, like p21 and p27; for example, it may affect the GSK-3 $\beta$  pathway that leads to cyclin D1 degradation [27], or the mTOR pathway that is associated with G1 arrest and involves a decrease in p21 levels [28]. Alternatively, the more prominent induction of apoptosis by compound **5** could be the reason for the caspase 3-induced cleavage of p21 protein [29]. Following 48 h of exposure to the compounds, the G1-arrested cells had undergone apoptosis without proceeding through the cell cycle. To the contrary, no

disturbances of the cell cycle were detected in MiaPaCa-2 cells. These results are in concordance with results of the MTT assay, which confirmed the selectivity of the compounds for the HeLa cell line.

Induction of apoptosis by compounds **3** and **5** was further confirmed using the Annexin-V assay. Although apoptosis was already present to some degree following 24 h of exposure to the compounds, massive cell death by apoptosis could be detected following 48 h of treatment. Activation of caspase-3, the most important downstream protease responsible for the execution of apoptosis [30], was measured following a 48 h exposure to each compound. The cleavage of PARP-1 by caspases is another important indicator of apoptosis [31]. At the 48 h time point, cleavage of PARP-1 was detected in cells treated by compound **5**, which was found to be a more potent inducer of apoptosis than compound **3**, while compound **3** did not induce PARP-1 cleavage at any time point investigated.

Cytotoxicity and the induction of apoptosis in tumor cells by selected cyano-substituted heteroaryles is consistent with previously published data that have shown cyano-compound structures to cause similar effects [11-13]. Our results revealed that the compounds block the cell cycle of HeLa cells following 24h of treatment, which is followed by apoptotic cell death. The aim of this study was to elucidate the mechanism(s) by which the compounds trigger apoptosis and then to relate these findings to compound structure and HeLa sensitivity; to do this, computational data analyses were carried out.

The results from the bioinformatics analysis revealed two interesting findings; 1) the cyano-substituted heteroaryles may act as mitotic inhibitors, and 2) HeLa/HEp-2 cells differ from the cyano-compound-insensitive tumor cell lines in their expression of locomotion-related genes. This suggested that following treatment with the cyano-compounds, the HeLa cells would show changes in their expression/function of intracellular actin and tubulin, as well as other proteins involved in cell migration and organization of the cytoskeleton [32]. Furthermore, cell cycle arrest and the induction of apoptosis are caused by such changes [33]. Indeed, both of the selected compounds inhibited the migration of HeLa cells following a 24 h exposure to the compounds. Staining of intracellular actin and tubulin revealed disruption of the cytoskeletal network, but only after 48 h of treatment. This delay in the disruption of actin/tubulin raised the question of whether the effect may be a consequence of and not a cause of cell death. This issue will require additional experimentation in order to be resolved, such as measuring tubulin polymerization, the activation of RHO and RAC GTP-ases, and the migration of cells in a 3D matrix. These experiments are beyond the scope of the present study. Nevertheless, changes in the migration rate, cell shape and polarity, and general

organization of the actin/tubulin filaments following treatment with the compounds were further substantiated by the analysis of protein expression levels. Compound **3** decreased the levels of the cytoskeletal filaments,  $\alpha$ -tubulin, and vimentin. The possibility that cells go through a process that is the reverse of the epithelial-to-mesenchymal transition (EMT) was tested by studying adhesion proteins, E-cadherin, N-cadherin, and p-120 catenin. EMT involves changes in cell phenotype, reflecting the transition of healthy cells into cancer cells, that are followed by changes in the metastatic potential and expression of various genes, and which are considered as markers of cancer cells [34,35]. If cells were to revert to a less metastatic phenotype, as well as possessing a reduced migratory potential, they should also express higher levels of E-cadherin and p-120 catenin, and lower levels of N-cadherin. Compound **3** did decrease the expression level of N-cadherin, but no differences were found in the expression of the two other markers; thus the EMT hypothesis is not substantiated. Surprisingly, compound **5** did not change the level of any tested protein. Another possibility, that would require additional analysis to investigate, is that changes to the cytoskeleton and migratory potential of treated HeLa cells are caused by the restoration of normal expression and localization of polarity proteins, *i.e.* Dlg and Scribble [36,37], which are severely imbalanced by HPV transformation. Such a scenario would imply that the compounds are able to interfere with HPV E6 oncogenic protein and would thus explain the special sensitivity of HeLa cells, however the results of the other experiments performed do not support this.

Since compound **5** only moderately influenced the integrity of the cytoskeleton yet exhibited a high apoptotic potential, the possibility that cellular ROS formation was affected was also tested. Disruption of the intracellular redox homeostasis, in particular by increases in the levels of ROS (a known effect of various antitumor lead compounds), results in the induction of apoptosis [38,39]. On the other hand, another category of potential chemotherapeutics that alter cellular redox homeostasis – antioxidants – have an even more beneficial effect upon the disease due to their therapeutic and preventive capacities [40]. Both compounds **3** and **5** demonstrated antioxidative properties, although compound **3** less so than compound **5**. This finding was not too surprising in light of reports that describe antioxidant properties of new agents structurally related to our compounds [41,42]. Interestingly, the reduced redox environment caused by antioxidant treatment stabilizes caspases and thus influences their activity and promotes the induction of apoptosis [43]. Furthermore, thiol antioxidants preferentially induce apoptosis in tumor cells [44], and epigallocatechin-3-gallate induces cell cycle arrest and apoptosis in a human keratinocyte carcinoma cell line, but not in

normal human keratinocytes [45]. The results herein presented are preliminary and additional studies are required, such as reduction potential measurements, and, in particular, measurement of GSH levels. Moreover, in light of our findings, experiments that would help to associate the induction of apoptosis and compound structure (*i.e.* the involvement of the cyano-substituents) with alterations in cell redox potential should be performed. Specifically, an activated cyano-group is toxic to a cell because it inhibits cytochrome c oxidase in the mitochondrial membrane [46], and release of cytochrome c and mitochondrial membrane potential changes are important features of apoptosis [47]. Interestingly, rhodanase – an enzyme that detoxifies the cyano-group – is also important for maintenance of a cell's redox potential [48]. Therefore, additional studies to investigate various aspects of the cytotoxicity of compound **5** should also be performed.

In conclusion, the cyano-compounds showed prominent cytotoxicity toward HeLa tumor cells by induction of severe apoptosis, and require further analysis in order to elucidate their antitumor mechanisms of action in more detail. Unfortunately, the identification of a unique, major mechanism of action was not confirmed, despite its anticipation due to the structural similarity of the compounds (*i.e.* the presence of the cyano-substituent) and their shared selectivity toward HeLa cells; some similarities in their mechanisms of action were identified however. Moreover, the question regarding what causes the compounds' selectivity toward HeLa cells remained unanswered. While compound **3** (a cyano-substituted naphthothiophene) reduced the expression of cytoskeletal proteins, compound **5** (a cyano-substituted thieno-thiophene-carboxanilide) inhibited formation of cellular ROS. The results suggest that the cyano-group, essential for cytotoxicity and selectivity, in different structural contexts may elicit different antitumor modes of action. Nevertheless, both of the selected compounds studied represent promising and interesting potential chemotherapeutics that deserve to be analyzed in greater depth.

### **Acknowledgments**

We thank Dr. Jaganjac for assistance with measurements of intracellular ROS, and to Dr. Čimbora-Zovko who kindly provided antibodies for cytoskeletal-study. We also thank to Dr. Ragland for helpful comments.

This study was supported by grants from the Ministry of Science, Education and Sports of the Republic of Croatia to MK (098-0982464-2514) and to TŠ (098-0000000-3168) and from Ministero dell'Istruzione, dell'Università e della Ricerca, Italy (PRIN 2008) to DL.

## References

1. Caleta I, Kralj M, Marjanovic M, Bertosa B, Tomic S, Pavlovic G, Pavelic K, Karminski-Zamola G (2009) Novel cyano- and amidinobenzothiazole derivatives: synthesis, antitumor evaluation, and X-ray and quantitative structure-activity relationship (QSAR) analysis. *J Med Chem* 52:1744-1756.
2. Hranjec M, Piantanida I, Kralj M, Suman L, Pavelic K, Karminski-Zamola G (2008) Novel amidino-substituted thienyl- and furylvinylbenzimidazole: derivatives and their photochemical conversion into corresponding diazacyclopenta[c]fluorenes. synthesis, interactions with DNA and RNA, and antitumor evaluation. *J Med Chem* 51:4899-4910.
3. Kemnitzer W, Kuemmerle J, Jiang S, Sirisoma N, Kasibhatla S, Crogan-Grundy C, Tseng B, Drewe J, Cai SX (2009) Discovery of 1-benzoyl-3-cyanopyrrolo[1,2-a]quinolines as a new series of apoptosis inducers using a cell- and caspase-based high-throughput screening assay. 2: Structure-activity relationships of the 4-, 5-, 6-, 7- and 8-positions. *Bioorg Med Chem Lett* 19: 3481-3484.
4. Ester K, Hranjec M, Piantanida I, Caleta I, Jarak I, Pavelic K, Kralj M, Karminski-Zamola G (2009) Novel derivatives of pyridylbenzo[b]thiophene-2-carboxamides and benzo[b]thieno[2,3-c]naphthyridin-2-ones: minor structural variations provoke major differences of antitumor action mechanisms. *J Med Chem* 52:2482-2492.
5. Jarak I, Kralj M, Suman L, Pavlovic G, Dogan J, Piantanida I, Zinic M, Pavelic K, Karminski-Zamola G (2005) Novel cyano- and N-isopropylamidino-substituted derivatives of benzo[b]thiophene-2-carboxanilides and benzo[b]thieno[2,3-c]quinolones: synthesis, photochemical synthesis, crystal structure determination, and antitumor evaluation. *J Med Chem* 48:2346-2360.
6. Jarak I, Kralj M, Piantanida I, Suman L, Zinić M, Pavelic K, Karminski-Zamola G (2006) Novel cyano- and amidino-substituted derivatives of thieno[2,3-b]- and thieno[3,2-b]thiophene-2-carboxanilides and thieno[3',2':4,5]thieno- and thieno[2',3':4,5]thieno [2,3-

c]quinolones: synthesis, photochemical synthesis, DNA binding, and antitumor evaluation. *Bioorg Med Chem*. 14:2859-2868.

7. Starcević K, Kralj M, Piantanida I, Suman L, Pavelić K, Karminski-Zamola G (2006) Synthesis, photochemical synthesis, DNA binding and antitumor evaluation of novel cyano- and amidino-substituted derivatives of naphtho-furans, naphtho-thiophenes, thieno-benzofurans, benzo-dithiophenes and their acyclic precursors. *Eur J Med Chem* 41:925-939.

8. Milazzo S, Lejeune S, Ernst E (2007) Laetrile for cancer: a systematic review of the clinical evidence. *Support Care Cancer* 15:583-595.

9. Park HJ, Yoon SH, Han LS, Zheng LT, Jung KH, Uhm YK, Lee JH, Jeong JS, Joo WS, Yim SV, Chung JH, Hong SP (2005) Amygdalin inhibits genes related to cell cycle in SNU-C4 human colon cancer cells. *World J Gastroenterol* 11:5156-5161.

10. Chang HK, Shin MS, Yang HY, Lee JW, Kim YS, Lee MH, Kim J, Kim KH, Kim CJ (2006) Amygdalin induces apoptosis through regulation of Bax and Bcl-2 expressions in human DU145 and LNCaP prostate cancer cells. *Biol Pharm Bull* 29:1597-1602.

11. Kemnitzer W, Kuemmerle J, Jiang S, Zhang HZ, Sirisoma N, Kasibhatla S, Crogan-Grundy C, Tseng B, Drewe J, Cai SX (2008) Discovery of 1-benzoyl-3-cyanopyrrolo[1,2-a]quinolines as a new series of apoptosis inducers using a cell- and caspase-based high-throughput screening assay. Part 1: Structure-activity relationships of the 1- and 3-positions. *Bioorg Med Chem Lett* 18:6259-64.

12. Kemnitzer W, Jiang S, Wang Y, Kasibhatla S, Crogan-Grundy C, Bubenik M, Labrecque D, Denis R, Lamothe S, Attardo G, Gourdeau H, Tseng B, Drewe J, Cai SX (2008) Discovery of 4-aryl-4H-chromenes as a new series of apoptosis inducers using a cell- and caspase-based HTS assay. Part 5: modifications of the 2- and 3-positions. *Bioorg Med Chem Lett* 18(2):603-607.

13. Saczewski F, Reszka P, Gdaniec M, Grünert R, Bednarski PJ (2004) Synthesis, X-ray crystal structures, stabilities, and in vitro cytotoxic activities of new heteroarylacrylonitriles. *J Med Chem* 47:3438-3449.

14. Saczewski F, Stencel A, Bieńczyk AM, Langowska KA, Michaelis M, Werel W, Hałasa R, Reszka P, Bednarski PJ (2008) Structure-activity relationships of novel heteroaryl-acrylonitriles as cytotoxic and antibacterial agents. *Eur J Med Chem* 43:1847-1857.
15. Hranjec M, Pavlovic G, Marjanovic M, Kralj M, Karminski-Zamola G (2010) Benzimidazole derivatives related to 2,3-acrylonitriles, benzimidazo[1,2-a]quinolines and fluorenes: Synthesis, antitumor evaluation in vitro and crystal structure determination. *Eur J Med Chem* 45:2405-2417.
16. Supek F, Kralj M, Marjanovic M, Suman L, Smuc T, Krizmanic I, Zinic B (2008) Atypical cytostatic mechanism of N-1-sulfonylcytosine derivatives determined by in vitro screening and computational analysis. *Invest New Drugs* 26:97-110.
17. Breiman L (2001) Random Forests. *Mach Learn* 45: 5-32.
18. Díaz-Uriarte R, Alvarez de Andrés S (2006) Gene selection and classification of microarray data using random forest. *BMC Bioinformatics* 7:3.
19. Strobl C, Boulesteix AL, Kneib T, Augustin T, Zeileis A (2008) Conditional variable importance for random forests. *BMC Bioinformatics* 9:307.
20. Segal E, Friedman N, Koller D, Regev A (2004) A module map showing conditional activity of expression modules in cancer. *Nat Genet* 36:1090-1098.
21. Rubin E (2006) List mania: interpreting microarray results with the L2L server. *Brief Bioinform* 7:121-122.
22. Aldridge GM, Podrebarac DM, Greenough WT, Weiler IJ (2008) The use of total protein stains as loading controls: an alternative to high-abundance single-protein controls in semi-quantitative immunoblotting. *J Neurosci Methods* 172:250-254.
23. Rosenkranz AR, Schmaldienst S, Stuhlmeier KM, Chen W, Knapp W, Zlabinger GJ (1992) A microplate assay for the detection of oxidative products using 2',7'-dichlorofluorescein-diacetate. *J Immunol Methods* 156:39-45.

24. Lacroix, M (2008) Persistent use of “false” cell lines. *Int. J. Cancer* 122:1–4.
25. Joseph JP, Grierson I, Hitchings RA (1989) Taxol, cytochalasin B and colchicine effects on fibroblast migration and contraction: a role in glaucoma filtration surgery? *Curr Eye Res* 8:203-215.
26. DeFilippis RA, Goodwin EC, Wu L, DiMaio D (2003) Endogenous human papillomavirus E6 and E7 proteins differentially regulate proliferation, senescence, and apoptosis in HeLa cervical carcinoma cells. *J Virol* 77:1551-1163.
27. Pontano LL, Diehl JA (2009) DNA damage-dependent cyclin D1 proteolysis: GSK3beta holds the smoking gun. *Cell Cycle* 8:824-827.
28. Yazbeck VY, Buglio D, Georgakis GV, Li Y, Iwado E, Romaguera JE, Kondo S, Younes A (2008) Temsirolimus downregulates p21 without altering cyclin D1 expression and induces autophagy and synergizes with vorinostat in mantle cell lymphoma. *Exp Hematol* 36:443-450.
29. Jin YH, Yoo KJ, Lee YH, Lee SK (2000) Caspase 3-mediated cleavage of p21WAF1/CIP1 associated with the cyclin A-cyclin-dependent kinase 2 complex is a prerequisite for apoptosis in SK-HEP-1 cells. *J Biol Chem* 275:30256-30263.
30. Porter AG, Jänicke RU (1999) Emerging roles of caspase-3 in apoptosis. *Cell Death Differ* 6:99-104.
31. Soldani C, Scovassi AI (2002) Poly(ADP-ribose) polymerase-1 cleavage during apoptosis: an update. *Apoptosis* 7:321-328.
32. Friedl P, Wolf K (2003) Tumour-cell invasion and migration: diversity and escape mechanisms. *Nat Rev Cancer* 3:362-374.
33. Hall A (2009) The cytoskeleton and cancer. *Cancer Metastasis Rev* 28:5-14.

34. Mani SA, Yang J, Brooks M, Schwaninger G, Zhou A, Miura N, Kutok JL, Hartwell K, Richardson AL, Weinberg RA (2007) Mesenchyme Forkhead 1 (FOXC2) plays a key role in metastasis and is associated with aggressive basal-like breast cancers. *Proc Natl Acad Sci U S A* 104:10069-10074.
35. Guarino M, Rubino B, Ballabio G (2007) The role of epithelial-mesenchymal transition in cancer pathology. *Pathology* 39:305-318.
36. Humbert PO, Grzeschik NA, Brumby AM, Galea R, Elsum I, Richardson HE (2008) Control of tumourigenesis by the Scribble/Dlg/Lgl polarity module. *Oncogene* 27:6888-6907.
37. Thomas M, Narayan N, Pim D, Tomaić V, Massimi P, Nagasaka K, Kranjec C, Gammoh N, Banks L (2008) Human papillomaviruses, cervical cancer and cell polarity. *Oncogene* 27:7018-7030.
38. Circu ML, Aw TY (2010) Reactive oxygen species, cellular redox systems, and apoptosis. *Free Radic Biol Med* 48:749-762.
39. Jang JH, Lee TJ, Yang ES, Min DS, Kim YH, Kim SH, Choi YH, Park JW, Choi KS, Kwon TK (2010) Compound C sensitizes Caki renal cancer cells to TRAIL-induced apoptosis through reactive oxygen species-mediated down-regulation of c-FLIP(L) and Mcl-1. *Exp Cell Res* 316: 2194 – 2203.
40. Foti MC, Sharma SK, Shakya G, Prasad AK, Nicolosi G, Bovicelli P, Ghosh B, Raj HG, Rastogi RC, Parmar VS (2005) Biopolyphenolics as antioxidants: Studies under an Indo-Italian CSIR-CNR project. *Pure Appl Chem* 77:91–101.
41. Pinto-Basto D, Silva JP, Queiroz MJ, Moreno AJ, Coutinho OP (2009) Antioxidant activity of synthetic diarylamines: A mitochondrial and cellular approach. *Mitochondrion* 9:17–26.
42. Ferreira IC, Queiroz MJ, Vilas-Boas M, Estevinho LM, Begouinb A, Kirsch G (2006) Evaluation of the antioxidant properties of diarylamines in the benzo[b]thiophene series by free radical scavenging activity and reducing power. *Bioorg Med Chem Lett* 16:1384-1387.

43. Brash DE, Havre PA (2002) New careers for antioxidants. *Proc Natl Acad Sci U S A* 99:13969-13971.
44. Havre PA, O'Reilly S, McCormick J, Brash DE (2002) Transformed and Tumor-derived Human Cells Exhibit Preferential Sensitivity to the Thiol Antioxidants, N-Acetyl Cysteine and Penicillamine. *Cancer Res* 62:1443–1449.
45. Mukhtar H, Ahmad N (1999) Green Tea in Chemoprevention of Cancer. *Toxicol Sci* 52:111-117.
46. Leavesley HB, Li L, Prabhakaran K, Borowitz JL, Isom GE (2008) Interaction of Cyanide and Nitric Oxide with Cytochrome c Oxidase: Implications for Acute Cyanide Toxicity. *Toxicol Sci* 101:101-111.
47. Li M, Wang A-J, Xu J-X (2008) Redox State of Cytochrome c Regulates Cellular ROS and Caspase Cascade in Permeabilized Cell Model. *Protein Pept Lett* 15:200-205.
48. Sabelli R, Iorio E, De Martino A, Podo F, Ricci A (2008) Rhodanese–thioredoxin system and allyl sulfur compounds: Implications in apoptosis induction. *FEBS J* 275:3884-3899.